2005 American Control Conference
June 8-10, 2005. Portland, OR, USA

Robust Control Design for a Wheel Loader Using Mixed Sensitivity H-infinity and Feedback Linearization Based Methods

Roger Fales and Atul Kelkar

Abstract— **The existing industry practices for the design of control systems in construction machines primarily rely on classical designs coupled with ad-hoc synthesis procedures. Such practices lack a systematic procedure to account for invariably present plant uncertainties in the design process as well as coupled dynamics of the multi-input multi-output (MIMO) configuration. In this paper, an H_∞ based robust control design combined with feedback linearization is presented for an automatic bucket leveling mechanism of a wheel loader. With the feedback linearization control law applied, stability robustness is improved. A MIMO nonlinear model for an electro-hydraulically actuated wheel loader is considered. The robustness of the controller designs are validated by using analysis and by simulation using a complete nonlinear model of the wheel loader system.**

I. Introduction

In this work, a model of an electro-hydraulically controlled wheel loader is considered which includes uncertainty, is highly nonlinear. This necessitates consideration of robust stability in the design of the control system. An H_∞ design will be applied for two cases. One is with the basic plant model. The other is with the model augmented with a feedback linearization control law. The objective of the control system design is to track a coordinated linkage motion reference called "level lift". H_∞ norm analysis will be used to evaluate the stability robustness given variations in the hydraulic model parameters, fluid bulk modulus and valve discharge coefficient.

In an example of related work by other researchers, H_2 and H_∞ control designs were presented for a hydraulic power train in [7]. However, these efforts focussed on systems which lack some of the characteristics that are found in typical mobile hydraulic machines such as the load sensing pump presented in this work. A control design based on feedback linearization was developed for a load sensing hydraulic system[11]. However that system was for the control of a single rotary motor using a servo valve rather than a multiple valve system. The nonlinear control technique known as feedback linearization was evaluated by some researchers in recent years for use with hydraulic control systems [9]. The analysis of the robust stability with respect to parameter variations and the application of feedback linearization to multiple valve functions are unique to this work.

TABLE I
NOMENCLATURE

Symbol	Description
P_{LS}	Load sense pressure at valve
P_T	Tank pressure
i_1	Tilt valve solenoid current
i_2	Lift valve solenoid current
x	State vector
$A(s_n)_{PA,n}$	Orifice area funct. of s, valve n, vol. P (pump out.) to A
Q_v	Sum of flows from pump to valves
$A_{cyA,n}$	Cylinder n area on side A
$V_{A,n}(x_n)$	Volume of cylinder n on side A
C_d	Valve discharge coefficient
$Q_{AB,n}$	Flow from "A" to "B" for
	the n^{th}function
M	Inertia matrix for linkage
h	Centrifugal, Coriolis, and potential force term for linkage
G_p	Pump displacement control gain
G_v	Valve actuator gain
r	Ref. input for tracking control
b	Viscous friction coefficient
β	Fluid bulk modulus
ρ	Fluid density
C_d	Orifice discharge coefficient
K_{LP}	Leakage factor for pump
ω_p	Pump speed
V_p	Pump outlet volume
P_{margin}	Pump margin pressure setting
τ_v	Valve time constant
τ_p	Pump time constant
θ_1	Boom lift angle w.r.t. chassis
θ_{21}	Bucket tilt angle w.r.t. boom
θ_2	Bucket angle w.r.t. chassis
y	Plant output vector
y_m	Measurement vector
y_{fn}	Force of cylinder n
u	Plant input vector
$G(s)$	Linearized plant

II. Model

The overall model consists of hydraulics (cylinders, valves, pump, etc.) and two degree of freedom linkage (1). The dynamic equations for the linkage and hydraulic system are given with some detail in [3]. The equations can be combined to form a MIMO state space system. The state vector, x, is defined in Table II. The input is the current in two valve solenoids as follows: $u = [i_1, i_2]^T$. The output is given as, $y = [\theta_1, \theta_{21}]$. The states of the model are summarized in table II. The dynamic equations for the linkage and electrohydraulic system in terms of state variables can be written as follows:

$$\begin{aligned} \dot{x}_1 &= x_3 \\ \dot{x}_2 &= x_4 \\ \begin{bmatrix} \dot{x}_3 \\ \dot{x}_4 \end{bmatrix} &= M^{-1}(\tau(x_9, x_{10}, x_{12}, x_{13}) - h(x_1, x_2, x_3, x_4)) \end{aligned}$$

This work was supported by John Deere

R. Fales is an assistant professor at the Department of Mechanical & Aerospace Engineering, University of Missouri - Columbia, Columbia, MO 65211, USA falesr@missouri.edu

A. Kelkar is an associate professor at the Department of Mechanical Engineering, Iowa State University, Ames, IA 50011, USA akelkar@iastate.edu

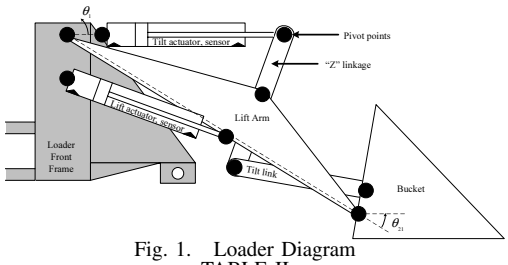

Fig. 1. Loader Diagram

TABLE II

PLANT STATES

State	Symbol	Description	Units
1	x_1	Tilt cylinder position	cm
2	x_2	Lift cylinder position	cm
3	$\dot{x}_1$	Tilt cylinder velocity	cm/sec
4	$\dot{x}_2$	Lift cylinder velocity	cm/sec
5	P_p	Pump pressure	MPa
6	D_p	Pump displacement	cm^3
7	P'_{LS}	Load sense pressure	MPa
8	s_1	Tilt function spool valve position	mm
9	$P_{A,1}$	Tilt cylinder cap end pressure	MPa
10	$P_{B,1}$	Tilt cylinder rod end pressure	MPa
11	s_2	Lift function spool valve position	mm
12	$P_{A,2}$	Lift cylinder cap end pressure	MPa
13	$P_{B,2}$	Lift cylinder rod end pressure	MPa

$$
\begin{aligned}
\dot{x}_5 &= \frac{\beta}{V_p}(\omega_p x_6/2\pi - x_5 K_{Lp} - (Q_{PA,1}(x_5,x_8,x_9) + \\
&\quad Q_{PB,1}(x_8,x_{10}) + Q_{PA,2}(x_5,x_{11},x_{12}) + \\
&\quad Q_{PB,2}(x_5,x_{11},x_{13})))\\
\dot{x}_6 &= [x_7 - x_5 + P_{margin}]G_p\\
\dot{x}_7 &= (max(x_9,x_{10},x_{12},x_{13}) - x_7)1/\tau_p\\
\dot{x}_8 &= (-x_8 + G_v u_1)1/\tau_v\\
\dot{x}_9 &= \frac{\beta}{V_{A,1}(x_1)}(Q_{PA,1}(x_5,x_8,x_9) + \\
&\quad Q_{TA,1}(x_8,x_9) - \dot{V}_{A,1}(x_3))\\
\dot{x}_{10} &= \frac{\beta}{V_{B,1}(x_1)}(Q_{PB,1}(x_8,x_{10}) + \\
&\quad Q_{TB,1}(x_8,x_{10}) - \dot{V}_{B,1}(x_3))\\
\dot{x}_{11} &= (-x_{11} + G_v u_2)1/\tau_v\\
\dot{x}_{12} &= \frac{\beta}{V_{A,2}(x_2)}(Q_{PA,2}(x_5,x_{11},x_{12}) + \\
&\quad Q_{TA,2}(x_{11},x_{12}) - \dot{V}_{A,2}(x_4))\\
\dot{x}_{13} &= \frac{\beta}{V_{B,2}(x_2)}(Q_{PB,2}(x_5,x_{11},x_{13}) + \\
&\quad Q_{TB,2}(x_{11},x_{13}) - \dot{V}_{B,2}(x_4)) \qquad (1)
\end{aligned}
$$

The flows in each valve are given by the standard orifice equation [5]. For example, the flow across the orifice area, $A_{PA,1}$, in a hydraulic valve 1 is given by

$$Q_{PA,1} = A_{PA,1}(x_8)C_d\sqrt{2|x_5 - x_9|/\rho}sgn(x_5 - x_9) \quad (2)$$

The operating point for linearization of the model is chosen such that the valves are shifted from the zero position in the negative direction. With operating point selected in this way, the boom raises while the bucket curls upward. It should be noted that the linearization result would change depending on the selection of a different operating point.

After linearizing the plant, input and output scalings, D_u, and D_y, respectively, were selected such that the expected input and output magnitudes were less than or equal to unity for the scaled plant: $G(s) = D_y^{-1}G_{unscaled}(s)D_u$.

The maximum and minimum singular values for the plant were plotted over a large frequency range as shown in Fig. 2. The plot shows that the system has a high gain at low frequencies indicating that low steady state error should be achieved with a closed-loop control system. Another observation is that the system appears to have resonant peaks at approximately 10 Hz and 20 Hz.

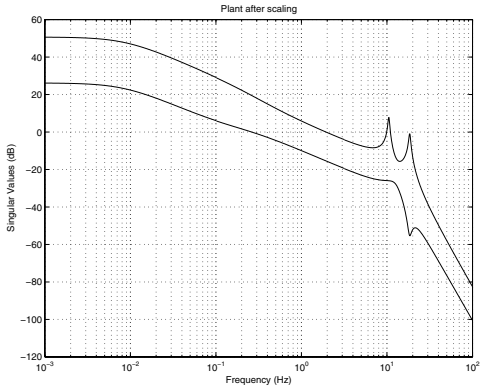

Fig. 2. Singular value plot of the plant after scaling

III. UNCERTAINTY

The effective bulk modulus of the system can be difficult to determine whether by measurement or analytically due to entrained air and container effects. The effective bulk modulus is a parameter which can vary by as much as 50 percent [9]. Uncertainty in the valve area geometry due to manufacturing variations can be captured as variations of the discharge coefficient by considering discharge coefficient as a gain on the pressure flow relationship or the valve area. A family of linearizations of the system model, G, was created with each having the same operating point but different randomly selected values within an interval of $\pm 50\%$ of nominal bulk modulus and discharge coefficient (Fig. 3). The nominal values of the parameters are $C_d = .62$ and $\beta = 1.7 \times 10^9$ Pa. The plant description including

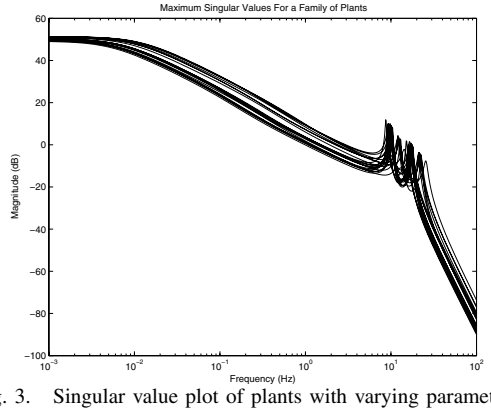

Fig. 3. Singular value plot of plants with varying parameters

uncertainty can be given as

$$G = G_{nom}(I + \mathbf{\Delta}), \quad (3)$$

where $\mathbf{\Delta}$ represents the uncertainty in the model. Let $\mathbf{\Delta} = \Delta W_i$ where Δ is the set of all model perturbations which are transfer matrices with the infinity norm less than or equal to one. The term, W_i becomes a weight in the form of transfer function matrix which bounds all of the possible perturbations of the plant model. The weight is plotted in

Fig. 4 along with the family of plant perturbations. Unmodeled dynamics, and plant variations due nonlinearities as the operating point changes are also important but not considered here.

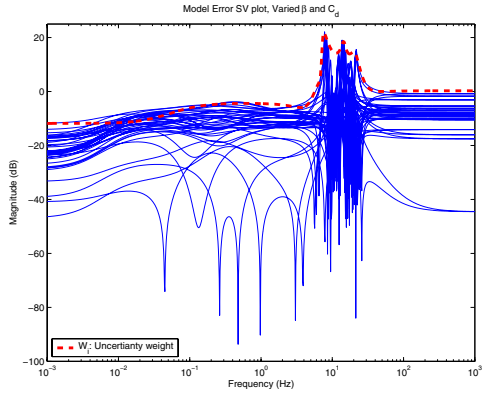

Fig. 4. Singular value plot of plant uncertainty and bounding weight for varied parameters, β and C_d

IV. Controller Design

A. Design Requirements

The goal of the controller design is to be able to lift the boom (or lift arm) at a desired rate while maintaining the bucket in a leveled position. This is a challenge for open-loop operation since the boom and bucket are coupled both in terms of the kinematics of the linkage and in terms of having a common hydraulic system power source. When the boom is raised to an angular position, θ_1, the relative angle of the bucket with respect to the boom must be, $\theta_{21} = -\theta_1$ for the bucket to be leveled.

Ramp inputs are found to be reasonable approximations of the level lift reference inputs. Therefore, a control requirement is to track ramp inputs for the tilt and lift functions with low tracking error. Another requirement is to have reasonably fast response to ensure high productivity. A bandwidth of 1.0 Hz is desired to meet the targeted speed of response.

The final requirement is robust stability. Any controller design should remain stable for known plant perturbations. Uncertainty in the plant is modeled as an input multiplicative uncertainty. The uncertainty model is due to variations in parameters β and C_d as discussed earlier.

The controller, the plant, and the uncertainty model can be transformed into a standard form (Fig. 5) by manipulating the model. The robust stability conditions for this configuration are that the nominal plant is stable and the following inequality given in terms of the maximum singular value is satisfied. $\bar{\sigma}(N_{11}) < 1$.

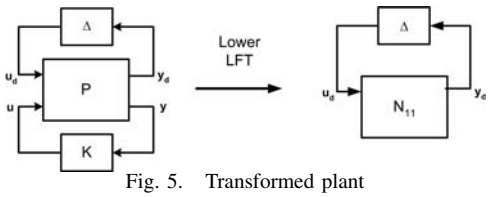

Fig. 5. Transformed plant

B. Mixed Sensitivity H_∞

1) Control Design: The H_∞ design presented here is based on shaping the sensitivity and complementary sensitivity transfer functions which are given as, $S = (I + GK)^{-1}$ and $T = GK(I + GK)^{-1}$, respectively; where, G is the nominal plant model. To reduce the possibility of actuator saturation, the transfer function KS is also considered. For an H_∞ design, refer to the block diagram which gives the structure of the control system in Fig. 6[6]. The closed-loop plant dynamics can be cast into the form,

$$\begin{Bmatrix} z_1 \\ z_2 \\ z_3 \\ v \end{Bmatrix} = \begin{bmatrix} W_p & -W_pG \\ 0 & W_tG \\ 0 & W_u \\ I & -G \end{bmatrix} \begin{Bmatrix} r \\ u \end{Bmatrix}, \tag{4}$$

where r is the reference input (desired boom and bucket angles), v is the input to the controller, and $z_{1,2,3}$ are weighted errors. An H_∞ controller is designed to minimize the following cost function,

$$\left\| \begin{matrix} W_pS \\ W_tT \\ W_uKS \end{matrix} \right\|_\infty \leq \gamma, \tag{5}$$

where K is the resulting controller. The control input to the plant is given by $u = K(r - y_m)$. The weighting matrices, W_p and W_t, are set to

$$W_p = \begin{bmatrix} W_{p1} & 0 \\ 0 & W_{p2} \end{bmatrix}, W_t = \begin{bmatrix} W_{t1} & 0 \\ 0 & W_{t2} \end{bmatrix}, \tag{6}$$

$$W_u = \begin{bmatrix} 1 & 0 \\ 0 & 1 \end{bmatrix}$$

with

$$W_{p1} = W_{p2} = \frac{0.667(s+9.425)^2}{(s+0.4417)^2}$$

$$W_{t1} = W_{t2} = \frac{31.62(s+5.027)}{(s+238.4)}.$$

It is desired to have good tracking of step and ramp signals. Therefore a small gain needed on S at low frequencies (unity gain on T at low frequencies, $T = I - S$). A double integrator approximation is used for tilt and lift performance weight, W_p, which is a weight on S (see Fig. 7). The slope of W_p is 40 dB/decade at low frequencies and leveling off at very low frequencies. The system should not be effected by high frequency signals either from the reference input or from noise so the weight on T, which is given by W_t, is chosen to have a low gain at high frequencies. Since the reference input for the lift function is from a joystick, the bandwidth on T could be chosen such that operator induced oscillation is attenuated. In this case the weights, W_p and W_t, have been chosen with a bandwidth of about 1.4 Hz. An H_∞ design was synthesized using a standard H_∞ design optimization procedure [8]. The design process yielded a two input two output controller with $\gamma = 1.77$.

The singular value plots of the resulting sensitivities S and T are given in Fig. 7. The bandwidth is greater than desired and the peaks are low (< 1 dB) indicating good stability robustness.

2) Robustness: The robustness analysis for varying plant parameters, β and C_d, is given in Fig. 8 for the H_∞ controlled system. The robust stability condition is violated between about 6 and 25 Hz.

3) Simulations: A simulation of the level lift tracking task with the nonlinear model shows that both functions, lift and tilt, track commanded input well with the H_∞ controller (Fig. 9). The tilt tracking error is very low. This may be

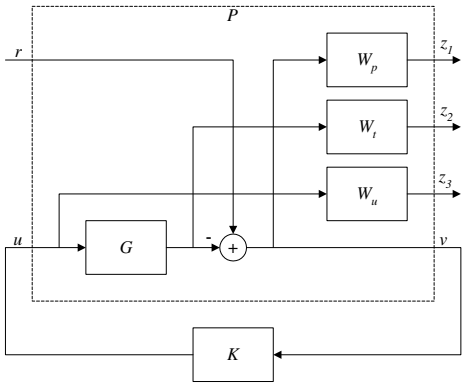

Fig. 6. Plant with Sensitivity Weights

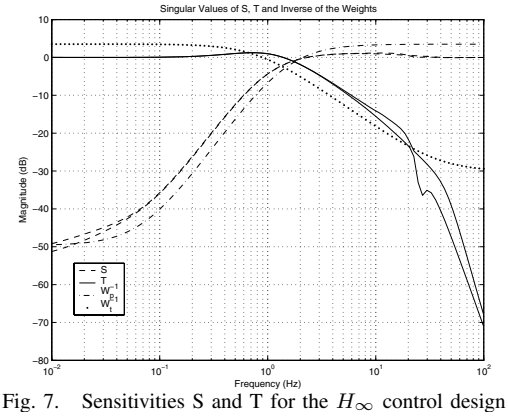

Fig. 7. Sensitivities S and T for the H_∞ control design

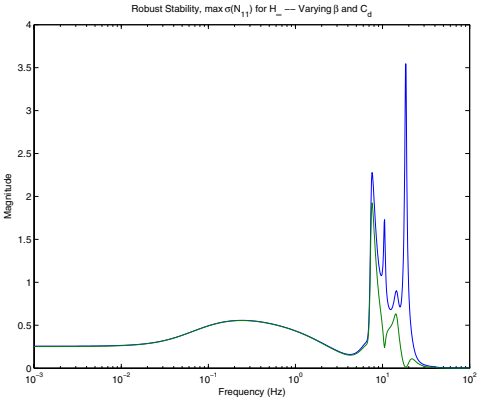

Fig. 8. Robust stability for H_∞ controlled system, varying parameters attributed to the selection of the performance weight, W_p. There is an initial jump in the tilt error.

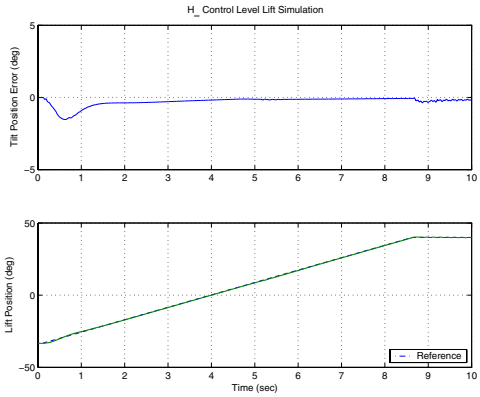

Fig. 9. Level lift simulation result using H_∞ and the nonlinear model

C. Feedback Linearization

The only nonlinear portion of the dynamics considered in the feedback linearization is the relationship between the spool valve position and the pressure within the hydraulic cylinders. In this section, the input-output feedback linearization was developed for the tilt and lift pressure dynamics. First, the feedback linearization control law for the tilt pressure system which gives a linear relationship between cylinder forces and the inputs is developed. A linearization is given for the plant including the feedback linearization control law. Finally, a tracking control system is developed.

1) Control Law: To achieve an input-output linearization for the tilt pressure system, the output of load force,

$$y_{f1} = A_{cy1}(x_9 - \alpha_1 x_{10})$$

is chosen. Recall that states x_9 and x_{10} correspond to the cylinder pressures and α_1 is the ratio of rod and cap end cylinder areas; therefore y_{f1} is the net force due to the pressure in the cylinder. The input to the system is the input valve position. The goal is to obtain a linear relationship between the valve position and the force on the hydraulic cylinder once the control law is applied. To simplify the control law and eliminate the need for velocity measurements an alternative output is chosen similar to the one given above [10]:

$$y_{f1} = A_{cy1}(\tilde{x}_9 - \alpha_1 \tilde{x}_{10}) \tag{7}$$

The the states denoted by $\tilde{x}_9$ and $\tilde{x}_{10}$ are from the following transformation:

$$\begin{aligned} \tilde{x}_9 &= x_9 + \beta \ln(V_0 + A_{cy1} x_1) \\ \tilde{x}_{10} &= x_{10} + \beta \ln(V_0 + \alpha_1 A_{cy1}(x_{m1} - x_1)) \end{aligned} \tag{8}$$

After taking the time derivative of y_{f1} the valve position, an expression for $\ddot{y}_{f1}$ is obtained and set equal to v_1 which will later become the new control input. The valve position, x_8, can then be solved for. Within the valve actuators bandwidth, the input current, u_1, is approximately equal to the spool position divided by G_v. Therefore, the input-output linearizing control law is given by

$$u_1(t) \approx x_8 \frac{1}{G_v} = \frac{1}{G_v \sqrt{2}\,\beta\, A_{cy1}\, C_d} \times \frac{v_1(t)}{\left(-\frac{K_{PA1}\sqrt{\frac{x_5(t)-x_9(t)}{\rho}}}{V_0 + A_{cy1}\, x_1(t)} - \frac{K_{TB1}\,\alpha_1\sqrt{\frac{-P_T+x_{10}(t)}{\rho}}}{V_0 + A_{cy1}\,\alpha_1\,(x_{m1}-x_1(t))} \right)}$$

for $u_1 < 0$ and by

$$u_1(t) \approx x_8 \frac{1}{G_v} = \frac{1}{G_v \sqrt{2}\,\beta\, A_{cy1}\, C_d} \times \frac{v_1(t)}{\left(-\frac{K_{TA1}\sqrt{\frac{-P_T+x_9(t)}{\rho}}}{V_0 + A_{cy1}\, x_1(t)} - \frac{K_{PB1}\,\alpha_1\sqrt{\frac{x_5(t)-x_{10}(t)}{\rho}}}{V_0 + A_{cy1}\,\alpha_1\,(x_{m1}-x_1(t))} \right)}$$

for $u_1 > 0$. The new cylinder force dynamics are given by:

$$\dot{y}_{f1} = v_1 \tag{9}$$

The force imparted on the linkage due to the hydraulic pressure is

$$F_1 = y_{f1} + A_{cy1}\beta(\ln(V_0 + A_{cy1}x_1) + \tag{10}$$

$$\alpha_1 \ln(V_0 + \alpha_1 A_{cy1}(x_{m1} - x_1))).$$

The last part of equation 10 is nonlinear because of the simplification made in y_{f1} using equation 8.

The control law has no singularities which appear in the normal operating range of the system. The control law accounts for the varying pump pressure which is somewhat unique to a load sensing system. The nonlinear volume effect on the hydraulic stiffness has been eliminated. Also significant, the nonlinear pressure flow relationship has been eliminated from the system dynamics.

A feedback linearization can also be developed for the lift function in a way similar to the tilt function previously given above. The output in this case is

$$y_{f2} = A_{cy2}(\tilde{x}_{12} - \alpha_2 \tilde{x}_{13}). \tag{11}$$

The input-output linearizing control law for the lift function is given by

$$u_2(t) \approx x_{11}\frac{1}{G_v} = \frac{1}{G_v\sqrt{2}\,\beta\,A_{cy2}\,C_d} \times \frac{v_2(t)}{\left(-\frac{K_{PA2}\sqrt{\frac{x_5(t)-x_{12}(t)}{\rho}}}{V_0+A_{cy2}\,x_2(t)} - \frac{K_{TB2}\,\alpha_2\sqrt{\frac{-P_T+x_{13}(t)}{\rho}}}{V_0+A_{cy2}\,\alpha_2\,(xm2-x_2(t))}\right)}$$

for $u_2 < 0$ and by

$$u_2(t) \approx x_{11}\frac{1}{G_v} = \frac{1}{G_v\sqrt{2}\,\beta\,A_{cy2}\,C_d} \times \frac{v_2(t)}{\left(-\frac{K_{TA2}\sqrt{\frac{-P_T+x_{12}(t)}{\rho}}}{V_0+A_{cy2}\,x_2(t)} - \frac{K_{PB2}\,\alpha_2\sqrt{\frac{x_5(t)-x_{13}(t)}{\rho}}}{V_0+A_{cy2}\,\alpha_2\,(xm2-x_2(t))}\right)}$$

for $u_2 > 0$. The force imparted on the linkage due to hydraulic pressure in the lift cylinder is

$$F_2 = y_{f2} + A_{cy2}\beta(\ln(V_0 + A_{cy2}x_2) + \alpha_2 \ln(V_0 + \alpha_2 A_{cy1}(x_{m2} - x_2))). \tag{12}$$

With the feedback linearization for the tilt and lift functions, the new system input is

$$\left\{ \begin{array}{c} v_1 \\ v_2 \end{array} \right\} = \left[\begin{array}{c} K_{f1}(y_{f-des1} - y_{f1}) \\ K_{f2}(y_{f-des2} - y_{f2}) \end{array} \right] = \left[\begin{array}{c} K_{f1}(F_{des2} - A_{cy1}(x_9 - \alpha_1 x_{10})) \\ K_{f2}(F_{des2} - A_{cy2}(x_12 - \alpha_2 x_{13})) \end{array} \right]. \tag{13}$$

An outer loop control used for position tracking which is used to supply the desired force on each cylinder is given as,

$$\left\{ \begin{array}{c} F_{des1} \\ F_{des2} \end{array} \right\} = K \left\{ \begin{array}{c} e_1 \\ e_2 \end{array} \right\} + F_{grav},$$

where, K is the outer loop controller gain, F_{grav} is a force vector used to compensate for gravitaty, and e_1 and e_2 are the position tracking errors for tilt and lift. The structure of the controller can be seen in Fig. 10.

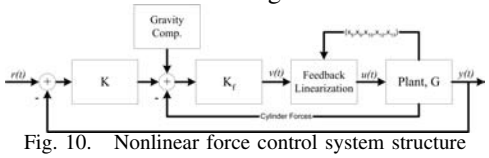

Fig. 10. Nonlinear force control system structure

2) Modified Plant Dynamics: It is hoped that the feedback linearization with force control will change the system dynamics in a such a way that the standard linear control methods can be more effective. This means that a new linearization needs to be found which incorporates the feedback linearization and force control. Therefore a new plant on which linear control design can be based has been taken as the "inner loop" system in Fig. 10. The new plant will be referred to as G'.

The linearization operating point has been selected to be the same as the one used for the linearization presented for the original model. The linearized and scaled plant, G', frequency response in the form of a singular value plot is given in Fig. 11. Note that the system no longer has the magnitude peaks near 10 to 20 Hz as the original plant did in Fig. 2. Since the feedback linearization and force control changes the system dynamics, a new analysis of plant uncertainty is needed. The singular value plot of the modified plant error due to variations in the bulk modulus and discharge coefficient is given in Fig. 12. The error was found in the same way as in the Model section. The new function (given on the plot) that bounds the error for use in the robust stability analysis will be referred to as W_i'. A comparison to Fig. 4 shows that the peak on the uncertainty is much lower for the system with feedback linearization and force control in comparison to the original plant.

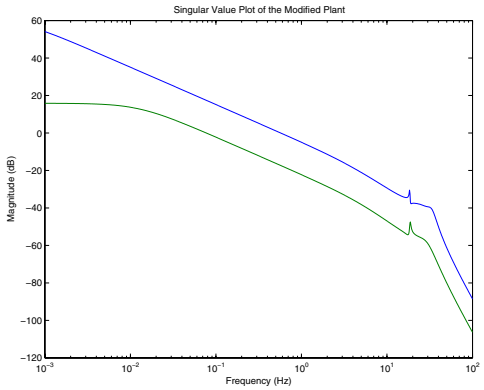

Fig. 11. Nonlinear force control system frequency response

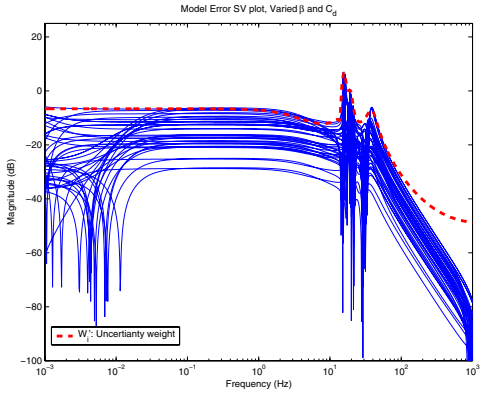

Fig. 12. Family of input multiplicative errors for the Nonlinear force control system

3) Outer Loop H_∞ Control Design: The mixed sensitivity H_∞ design procedure given earlier in this work

can be used with little modification to design an outer loop control for the plant with the feedback linearization force control. Since all of the design objectives remain the same, the design weights do not need to change. The only difference required is to used the modified plant, G' due to the feedback linearization in the design process.

Applying the previously discussed design weights in the mixed sensitivity H_∞ design process to the new model yielded a new feedback control system. The sensitivity, S, and complementary sensitivity, T, frequency responses are given in Fig. 13 along with the design weights. It can be concluded by examining the plots that the desired bandwidth appears to have been met. Also, stability robustness is good because the peaks on the plots of S and T are low.

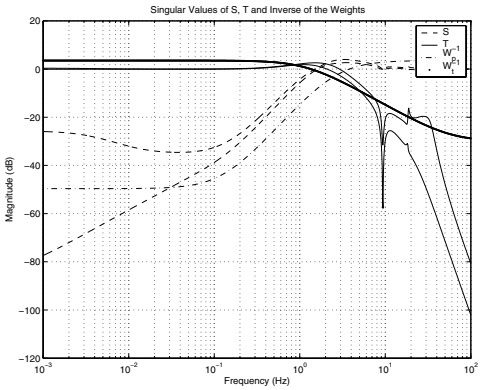

Fig. 13. Nonlinear/H_∞ force control system sensitivity frequency responses

4) Robustness of the Modified Plant with H_∞ Control: When robustness to varying plant parameters is being considered, the description of the model uncertainty, W_i' based on the modified plant, G', is used. The new robustness analysis for varying plant parameters, β and C_d, is given in Fig. 14. Clearly the robust stability condition is not violated which is a very significant achievement. Comparing this result to the result for the unmodified plant (see Fig. 8) indicates that the robustness problems are much less severe for the modified plant. The feedback linearization reduced the high frequency peak of the robust stability norm by 97% and the max by 86% for the parametric uncertainty.

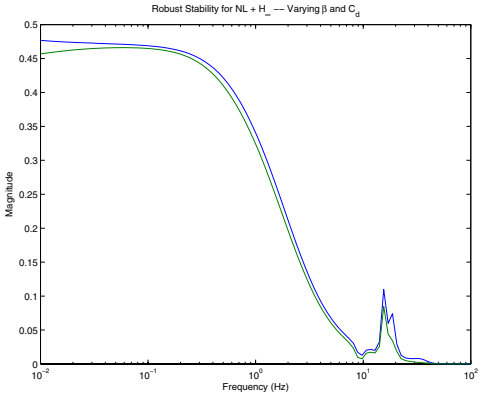

Fig. 14. Robust stability of the NL force - H_∞ controlled system with varying parameters

5) Simulation Results: The following simulations are responses to the level lift reference input (Fig. 15) with the nonlinear plant. In this case the tracking error is quite small but some oscillation is present in the margin pressure. The initial jump in tilt error is smaller than the case without the feedback linearization.

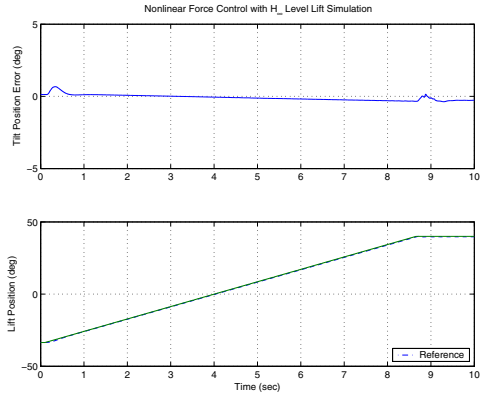

Fig. 15. Level lift simulation, H_∞ and nonlinear force control

V. Comparison and Summary

Linear controller designs were developed based on H_∞ methods with two cases: one with and one without a feedback linearization control law. Simulations show that the nonlinear nature of the wheel loader affects the performance of the linear control design. The H_∞ design without the feedback linearization provided an acceptable level lift performance with the nominal nonlinear model. A singular value analysis of the robustness of the H_∞ design showed that the linear control design was not robust to the uncertainty due to variations in the parameters, C_d and β. As expected, by accounting for the plant nonlinearities in the feedback linearization control design, the robustness was improved since the nonlinear control design passed the robust stability test while linear design did not.

References

[1] Burl, J., 1999, *Linear Optimal Control*, Addison-Wesley, Menlo Park.

[2] Chen, C.T., 1999, *Linear System Theory and Design*, Oxford University Press, New York.

[3] Fales, R.; A. Kelkar; E. Spencer; F. Wagner and K. Chipperfield, *Modeling and Control of a Construction Machine with a Human-in-the-Loop Assessment in Virtual Reality* IMECE2003-41597 ASME IMECE, Wash., DC, 2003.

[4] Maciejowski, J.M., 1989, *Multivariable Feedback Design*, Addison-Wesley, Wokingham.

[5] Merritt, H.E., 1967, *Hydraulic Control Systems*, Wiley, New York.

[6] Skogestad, S.; I. Postlethwaite, *Multivariable Feedback Control Analysis and Design*, John Wiley and Sons, Chichester, 1996.

[7] Zhang, R.; Aleyne A.; Prasetiawan E., "Modeling and H_2/H_∞ MIMO Control of an Earthmoving Vehicle Powertrain", ASME Journal of Dyn. Sys., Meas. and Control, **124**, pp. 625-636, 2002.

[8] Balas, G. J., Doyle, J. C., Glover, K., Packard, A., and Simth, R., *Mu (μ)-Analysis Toolbox, for Use with MATLAB*, Mathworks, Inc., MUSYN Inc, 2001.

[9] Jelali, M., A. Kroll, *Hydraulic Servo Systems: Modelling, Identification and Control*, London: Springer-Verlag, 2003.

[10] Kugi, A., *Nonlinear Control Based on Physical Models: electrical, mechanical and hydraulic systems*, London: Springer-Verlag, 2001.

[11] Chiriboga, J., M. Thein, E.A. Misawa, "Input-output feedback linearization control of a load-sensing hydraulic servo system," Control Applications, Proceedings of the 4th IEEE Conference on, Pages: 910 - 915, 28-29 Sept., 1995.